CONF-8905148--1 CONF-8905148--1

DE89 013639

# FIELD STUDIES FOR DETERMINING THE CHARACTERISTICS AND DYNAMICS OF LOCAL CIRCULATIONS*



by

P.H. Gudiken - Lawrence Livermore Laboratory, CA
W.E. Clements - Los Alamos National Laboratory, NM
R.P. Hosker - ATTD/NOAA, TN
C.D. Whiteman - Wave Propogation Lab., Boulder, CO
R.L. Coulter - Argonne National Laboratory, IL
G.E. Start - ERL, Idaho



*Work supported by the U.S. Department of Energy, Office of Health and Environmental Research, under contract W-31-109-ENG-38.

(1)

# FIELD STUDIES FOR DETERMINING THE CHARACTERISTICS AND DYNAMICS OF LOCAL CIRCULATIONS

Paul H. Gudiksen, William E. Clements, Rayford P. Hosker, Jr., C. David Whiteman, William D. Neff, Richard L. Coulter and G. Eugene Start.

## INTRODUCTION

The U.S. Department of Energy sponsored Atmospheric Studies in Complex Terrain (ASCOT) program is designed to improve our understanding of the physical processes that govern pollutant dispersion in areas of complex terrain and to develop the technology needed to predict the air quality impact of pollutants released into terrain dominated flows. The focus of the program has been on the study of the characteristics of locally generated valley circulations with the primary emphasis being on evaluating the life-cycle of nocturnal cold air slope and valley flows. This phenomenon was selected on the basis of its importance for transporting pollutants from energy related facilities to population centers that are generally situated within valleys.

The program's field studies component, which is closely integrated with the modeling activities, provides the data needed to evaluate the characteristics and dynamics of locally generated valley circulations. The Geysers geothermal area in northern California, situated within the coastal-mountain range, was chosen as the initial field studies area. Three series of major field experiments were performed in this area during the period from 1979 to 1981. The initial studies were performed within the

Anderson Creek Valley, which was slated for geothermal energy development. This valley has the characteristics of a basin with a topographically restricted outflow region; a configuration that leads to pooling of the nocturnal valley flows within the basin. Two series of experiments were performed in this valley to acquire detailed information about the temporal and spatial characteristics of the nocturnal flows along the slopes, the circulations within the basin, and their interactions with the larger scale flows (Dickerson and Gudiksen 1983). The third series of experiments were performed within the Big Sulphur Creek Valley, situated immediately west of the Anderson Creek Valley, to evaluate the interactions of the geothermal power plant cooling tower plumes with the nocturnal valley flows, and to evaluate the structure of the nocturnal valley circulations in a different environmental setting. In concert with these studies, several smaller scale experiments were carried out over relatively simple slopes at Rattlesnake Mountain near Richland, Washington, Corral Gulch in western Colorado, and on Parajarito Mountain near Los Alamos, New Mexico.

Upon the completion of these experiments, the field studies were tranferred to the oil shale region of western Colorado to (1) test the transferability of the methodologies developed in The Geysers to a new environmental setting and (2) extend the studies to include not only the nocturnal valley flows, but also the morning transition and daytime flows. The Brush Creek Valley, situated about 50 km northeast of Grand Junction, was chosen as the study area. This is a long, straight and narrow valley whose nocturnal flows drain freely into the Roan Creek Valley in contrast with the pooling characteristics associated with the Anderson Creek Valley. Two series of major field experiments were carried out within the Brush Creek Valley in 1982 and 1984. Since then the focus has been on the analysis of the data generated by these experiments in regard to the surface energy budget, the structure of the nocturnal slope and valley flows and their interactions with the external meteorology, and the dispersion of pollutants entrained within the valley circulations.

These studies have truly reflected the multi-laboratory nature of the ASCOT program. The major experiments were performed by scientists from about a dozen DOE and NOAA laboratories and universities. The instrumentation deployed into the field included meteorological towers, tethersondes, acoustic sounders, rawinsondes, optical anemometers, lidar, and gaseous and particle tracers.

This paper provides an overview of some of the most salient features of valley circulations that influence the dispersion of pollutants. The emphasis is primarily on the most important characteristics that may be of interest to an emergency response manager who is responsible for developing emergency preparedness plans for facilities that may be influenced by valley circulations. The discussions will be centered on the results of the Anderson Creek Valley and the Brush Creek Valley studies to contrast the characteristics of a pooling valley with those of a draining valley. The paper also provides suggestions on the most critical measurements that are needed to define the behavior of the nocturnal valley flows that may be expected within any given valley.

## THE ANDERSON CREEK VALLEY FLOWS

The Anderson Creek Valley is a basin bounded by the 4400 m high Cobb Mountain on the north, by a 3200 m high ridge on the west and south, and by the 3600 m high Boggs Mountain on the east. The height of the center of the basin is approximately 1600 m. The Anderson, Gunning and Putah Creeks, which form the principal drainage areas, merge in the center of the basin with outflow toward the southeast. The entire valley is approximately 10 km wide.

The fundamental forcing process responsible for the development of nocturnal slope flows is radiative cooling of the ground surface. Under clear skies and during calm ambient winds, the radiational cooling may start about 2 to 3 hours before local sunset to produce the surface based temperature inversion that is needed to cause downslope air movement near the ground. Measurements of the temperature and wind structure of well-established nocturnal flows generated along the upper slopes of the valley revealed a surface based inversion within the lowest 30 to 60 m of the atmosphere. Below the temperature inversion, the winds are essentially downslope with a low level maximum of 1 to 2 m/s at a height that is roughly half the depth of the inversion. In the vicinity of the inversion and above it, the cross-slope component may increase with height depending on the direction and speed of the larger scale winds (Horst and Doran 1981).

As the flows from the higher elevations merge with those from other drainage areas and encounter irregular topographic features and forest canopies, very complicated flow structures may appear within the valley. This is illustrated by Orgill (1982) in Fig. 1, which shows the temperature distribution along a northwest-southeast cross-section of the Anderson Creek Valley for a period exhibiting strong downslope flows. Near the ridge only very shallow slope flows are formed. As the flows from adjacent slopes merge, they may flow over one another depending on their relative densities, and may collect within minor topograpic depressions. The flows deepen upon descent into the basin due to the continuous entrainment of air into the layer of slope flows and finally become involved in a basin wide circulation that appear to have the characteristics of a pool of cold air that slowly exits the valley toward the southeast. The horizontal and vertical dimensions of the pooling region is a function of the strength of the slope flows throughout the basin. The depth of this pool over the valley basin generally varies between 100 to 300 m and decreases with distance up the slopes. Above this pooling region and below the undisturbed outer flow region, lies a transition layer that is several hundreds of meters in depth. It is characterized by an isothermal temperature structure, and its interaction with the pool of cold air may result in rather complex and poorly understood wave interactions at the layer interfaces.

Figure 2 illustrates a typical surface flow pattern within the valley during a period of well-established nocturnal slope flows. This pattern is based on interpolation of extensive wind observations within the valley (Lange, 1985). Note the general northwesterly to northerly ridge flows that are aligned with and possibly reinforce the surface downslope flows predominating within the valley. Also note the northward wind component within the center of the valley. This is most likely due to outflow from one of the several small canyons draining into the main valley. In general, however, the slope flows converge within the basin with subsequent restricted outflow toward the southeast.

The nocturnal slope and basin flows observed within the Anderson Creek Valley are generally influenced to some extent by the larger scale flows. Besides the synoptic scale migratory systems, the principal influences are due to westerly sea breezes and descending upper-level northeasterly flows. Sea breeze intrusions, due to coastal and inland pressure differences, are not always easy to detect because the wind directions within the valley are still downslope. However, the near surface cooling rates within the valley become essentially uniform during periods of strong sea-breeze intrusions (Gudiksen and Walton, 1983) This is in marked contrast to the downslope gradient in the cooling rates that one observes during periods of strong slope flows when external flow interactions are minimal.

Occasional upper-level northeasterly flows over the ridges of the Anderson Creek Valley protruded into the valley to produce disruptions of well established slope flows on the exposed slopes. This phenomenon is illustrated in Fig. 3 by showing the locations of the bottom of the transition layer across the valley as a function of time. Note that on the sheltered side of the valley, the transition layer is deeper than on the downwind side; however, also note that it systematically moved downward throughtout the valley. This resulted in the northeast winds destroying the opposing nocturnal slope flows at progressively lower elevations on the exposed sloped surfaces (Orgill and Barr 1989). This observed behavior is consistent with the systematic change in the wavelenth of a nonlinear lee wave. If the wavelenth is close to the lateral dimensions of the hill, the flow will tend to follow the topography. If the wavelength is significantly different, the separation will not be suppressed. A relationship, developed for hills of moderate slope and for a narrow range of wavelengths, was able to provide indications of the occurrence of upper-level wind intrusions. Air flow will tend to follow the topography for conditions such that $2L \leq \Lambda < 5L$. In this relationship L is the half-width of the hill at half-height and ~~lambda~~ $\Lambda$ is the wavelenth of the lee wave given by $2\pi U/N$ where N is the Brunt-Vaisala freqency and U is the wind speed.

A series of tracer studies were performed to evaluate the pollutant dispersion characteristics of the slope flows and basin circulations within the valley. A perfluorocarbon tracer injected directly into the shallow nocturnal downslope flows along the western slopes typically produce the surface concentration distribution shown in Fig. 4 (Gudiksen et.al., 1984). The tracer, released at a height of 5 m above the surface over a one hour period, flowed downslope in a southeasterly direction until it entered the basin circulation. Note that the plume is initially rather narrow within the first 2 km of the source, and then appears to spread out horizontally at an accelerated rate with an attendent decrease in the concentrations as the plume becomes involved in the basin circulations. Vertical profiles of the tracer concentrations within the basin revealed that the tracer was mainly confined within the lowest 200 m. A second tracer, injected into the lower levels of the transition layer overlying the upper slopes, revealed considerable mixing between the transition layer flows and the underlying slope flows.

One of the major differences between meteorological and tracer measurements within complex terrain areas relative to those over flat terrain is the large spatial variability typically observed in complex terrain. This was illustrated by the perfluorocarbon tracer concentrations which varied by factors of 10 to 20 over distances of a few hundreds of meters at a distance of 6 km from the release site.

## THE BRUSH CREEK VALLEY FLOWS

The Brush Creek Valley, situated about 50 km northeast of Grand Junction, is one of a series of valleys that reside within the relatively flat Roan Plateau. It is a narrow 25 km long valley that is oriented in a northwest-southeast direction. The valley is roughly 650 m deep at the south end and exhibits 30-

40 degree sidewall slopes that have been cut by numerous small tributaries. The width of the valley floor gradually increases from about 300 m at mid-valley to about 700 m near its mouth.

Radiation and Surface Energy Budgets

Since the radiative processes responsible for cooling and heating the valley surfaces play a dominant role in determining the valley circulations, estimates of radiation and surface energy budgets were made during September - October 1984 at five sites on the valley floor, along the sidewalls, and on the ridgetop (Whiteman et. al., 1989). The diurnal variation of net radiation, ground heat flux, latent heat flux and sensible heat flux at the five sites are shown in Fig. 5 for a particular day in the fall. These fluxes are expected to be typical of clear fall days within deep, narrow valleys in dry continental settings. At the two valley floor sites (PNL and WPL) and the ridgetop (RDG) site, the net radiation was symmetric about the solar noon with the highest radiative gain being on the ridgetop (634 Wm-2). Strong asymmetries occurred on the east (E) and west (W) sidewall sites because the slope and aspect angles of the sidewalls markedly affect the timing and magnitude of the incoming radiation. Nocturnal net radiative losses at the measurement sites were typically 50 - 65 Wm-2 during clear sky conditions.

The daytime heat flux from the ground typically began an hour or more after local sunrise at all sites and ended before local sunset. These varied between 53 Wm-2 on the west sidewall and 139 Wm-2 measured at a moist site on the valley floor. The nocturnal ground heat fluxes were directed toward the surface at rates of 50 - 60 Wm-2; a magnitude comparable with the net nocturnal radiative energy loss from the surface, with the result that little energy was left for sensible and latent heat fluxes.

The latent heat fluxes measured at the five sites were small relative to those observed in moist climates (Oke,1978). The daytime fluxes were directly dependent upon the net incoming solar radiation and the soil moisture content. The values varied from 232 Wm-2 at the WPL site, situated in a moist meadow, to 79 Wm-2 along the dry east sidewall. The nocturnal latent heat fluxes, given in Fig. 5, are extremely small at all sites. The daytime sensible heat fluxes directly reflected the variation in incoming solar radiation at the individual measurement sites. Thus, the maximum values were observed on the sun exposed west sidewall during the morning (477 Wm-2) and on the east sidewall during the afternoon (565 Wm-2). This differential heating of the air above the two opposing sidewalls produces a cross-valley flow toward the more strongly heated sidewall. This is evidenced in the downvalley wind circulations observed during the morning transition period. In addition, these high sensible heat fluxes during the daytime are easily capable of destroying the typical nocturnal temperature inversions and to provide the energy necessary to develop the deep daytime convective boundary layer.

## Slope and Valley Flows

This radiative cooling and heating of the valley surfaces produce downslope and upslope flows along the valley sidewalls and within the tributaries. The nocturnal sidewall and tributary flows produce the observed downvalley flow system. Typical profiles of the diurnal characteristics of the sidewall flows are illustrated in Fig. 6. These were derived from measurements acquired from a meteorological tower situated on the northeast sidewall at about 110 m above the valley floor (Stone and Hoard 1989). Another tower on the southwest sidewall produced similar profiles. Even though the main nocturnal wind component is downvalley, a shallow downslope component is present. Its depth is typically less than 15 m and display a speed maximum of less than 1 m/s at a height of about 2 to 3 m above the surface. Shortly after the valley is exposed to the morning sun the slope flows weaken, and subsequently reverse to the upslope and upvalley directions. The nocturnal flows within the tributaries are very complex and their contribution to the main downvalley flows is not well known. Studies of tributaries within the Brush Creek Valley (Coulter, et. al. 1989; Porch, et. al. 1989; and Neff 1989) revealed that the flow out of a tributary is not simply proportional to its drainage area, but also depends on the exposure of the tributary slopes to the ambient winds as well as terrain features that often protrude from the tributary into the main valley. Thus, estimates of mass flux out of a single tributary have ranged from about 1 to 15% of the total mass of the main downvalley flow system.

The resulting nocturnal downvalley flow system may be characterized by the vertical cross-sectional views of the valley axis wind speeds, shown in Fig. 7 for the nighttime, morning transition, and daytime periods. The data in the figure were obtained by a Doppler Lidar that measured the winds along the valley axis (Post and Neff, 1986). The nocturnal flows revealed a downvalley jet centered about 100 m above the valley floor with a maximum wind speed of about 6 m/s. The downvalley flows extended to a height of about 400-500 m; above this level the ambient flows predominated. As the sun heated the western sidewall after sunrise, the flows weakened and the upward vertical motion produced by the heated surface induced the entire downvalley flow structure to be translocated over the west sidewall as shown in Fig. 7b. After the entire valley is heated by exposure to the sun, the downvalley flows continued to weaken and subsequently reversed to upvalley flow by mid-morning as depicted in Fig. 7c.

A detailed analysis of the vertical and horizontal cross-section of the nocturnal downvalley wind speed derived from several field experiments conducted within the Brush Creek Valley yielded the following "Prandtl-parabolic wind field" description (Clements, et. al. 1989)

$$U(y,z) = A u_m e^{-Bz/D} \sin(\pi z/D) [E + F(y/H)^2]$$

where $u_m$ is the maximum wind speed in the drainage flow, H = H(z), A = 3.2, B = 3.3, E = 0.95, and F = -0.85.

The vertical temperature structure in the valley is characterized by a strong surface based inversion (typically 3.2 K/100m) in the lowest 200 m overlain by a quasi-isothermal layer extending to above the ridgetop.

## Turbulence Characteristics

Turbulence measurements related to pollutant diffusion over complex terrain have been relatively limited. The interpretation of such measurements is a formidable task, complicated by factors such as limited and rapidly changing upwind fetches, tilting and distortion of streamlines, and problems of representativeness. This is illustrated in Fig. 8 by the high variability exhibited by the $\sigma_\theta$ values acquired during periods of strong radiatively induced slope flows within the Anderson, Big Sulphur, and Brush Creek valleys (Gudiksen 1989). The figure shows the medians of the hourly-averaged values obtained at each measurement site within the three valleys in order of height above the floor of the respective valleys. One notes that the $\sigma_\theta$ values span a range from about 15 to 40 degrees. Thus, the values typically exceed those reported over flat terrain for stable conditions by a factor of to 4. In general, the stations situated on the valley floor and along the lower slopes display the highest median values; while the ridge stations exhibit the lowest median values. This appears to be due to an inverse correlation with wind speed as indicated by comparing the $\sigma_\theta$ values with the median wind speed distribution also illustrated in Fig. 8. Thus, if one compares the median $\sigma_\theta$ values with the corresponding median wind speeds, one notes that the data may reasonably be fitted with the relationship $\sigma_\theta u = 0.7$ m/s, where u is the wind speed and $\sigma_\theta$ is in radians. This is based on the relationship $\sigma_\theta = \sigma_v/u$, where $\sigma_v$ is the standard deviation of the horizontal wind speed fluctuations, and assuming $\sigma_v$ to be constant.

The vertical distribution of turbulent energy was measured by means of a sonic anemometer suspended below a tethered balloon. The results indicated that the Richardson numbers over the center of the valley during a strong nocturnal downvalley flow period increased from about 0.1 near the surface to a maximum of about 20 near the center of the downvalley jet where the vertical gradient of wind speed is small. The applicability of these values to the vertical diffusion of a tracer injected into the nocturnal valley flows is not at all clear. The stability that one may infer from these high values is not consistent with observed diffusion of tracers discussed in a subsequent section of this report.

## Effects of External Meteorology

The two primary mechanisms by which the ambient atmosphere may influence the strength and depth of the locally-driven nocturnal slope and valley flows are (1) the reduction of the long-wave radiative cooling of the valley's sloping surfaces and (2) erosion of the upper part of the nocturnal valley flows by turbulent mixing with the larger scale flows above the valley. As illustrated in a previous section, the radiative cooling characteristics of sloping surfaces are dependent on the surface energy budget which may be influenced by atmospheric moisture and clouds, soil moisture, etc.

Orgill and Barr(1989) developed a heuristic model to account for these effects. The radiative component of this model is based on the ratio of the net outgoing long-wave radiation and the emitted long wave flux which is sensitive to the surface and upper air temperature, emissivity, precipitable water vapor, and clouds. The ratio, commonly referred to as the Angstrom ratio, expresses the leakage of long-wave energy through the atmospheric window. It is relatively large in dry air (0.2-0.4) and decreases toward zero due to cloudiness and increasing moisture content of the atmophere. Figure 9 depicts the nightly averaged depths of the nocturnal downvalley flows as a function of this ratio. The large amount of scatter suggests that although radiative cooling provides the basic driving function for the nocturnal valley winds, the total mass and depth of the flows are strongly modulated by other physical processes. One may consider the curve in Fig. 9 as an upper bound on the cool air flows that could develop in the absence of erosive effects of turbulent mixing. The observed points that fall below the curve might then represent the amplitude of the wind driven effects. The curve has been extended beyond the range of observations by assuming that an Angstrom ratio of zero denotes no radiational induced flows and a ratio of 0.2 corresponds to a flow domain that fills the valley.

The effect of the ambient winds on the depth of the nocturnal downvalley flows is demonstrated in Fig. 10 by a plot of the ridgetop wind speeds as a function of flow depths at various measurement sites. The intercept for a zero ridgetop wind speed suggests that in the absence of external wind influences the flow generated by radiational cooling will fill the valley. Conversely, the data also suggests that winds exceeding 9 m/s upvalley at the ridgetop may be sufficient to overcome the flows. Regression analysis of the data in Fig. 10 yields the relationship

$$H/H_o = (1 - 0.068v)$$

where H is the top of the valley flow domain, Ho is the average ridge height, and v is the wind speed at ridge height.

Tracer Dispersion

A series of perfluorocarbon tracer experiments were performed to evaluate the behavior of inert pollutants entrained in nocturnal valley flows and the subsequent ventilation of the pollutants out of the valley during the morning transition period (Gudiksen and Shearer 1989). These experiments consisted of the simultaneous release of three perfluorocarbon tracers over a roughly nine hour period that extended from midnight to the initiation of the daytime upslope flow reversal after the morning transition period. One tracer (PMCH) was released on the valley floor at a site situated 12 km upvalley, while the second tracer (PDCH) was released 200 m directly above the valley floor release site. The third tracer (PMCP) was released on the ridgetop within a shallow depression that drained into a small sidecanyon within the Brush Creek Valley. To illustrate the general behavior of the tracers, Fig. 11 shows the time and spatially varying PMCH tracer concentration distributions observed during one experiment. The figure depicts the distributions observed along a vertical cross-section of the valley at a distance of 8 km downvalley from the release site as well as the distribution along the valley's main axis. The nocturnal concentration distributions, shown in Figs. 11a and b indicate that the plume is almost totally confined within the lowest 250 m of the valley atmosphere with the highest concentrations at the surface. This distribution is reasonably constant throughout the night with relatively minor oscillations in the location of the plume center. This well-defined plume structure appears to exist all along the downvalley axis. However, as the sun heats the west sidewall of the valley shortly after sunrise, the initiation of the upslope flows cause the plume to ascend the heated sidewall and subsequently be ventilated out of the valley. This is demonstrated in Fig. 11c. As the ventilation process accelerates during the morning hours the concentrations decrease rapidly even though the tracer is still being released. By mid-morning the concentrations have decreased to about 10% of their nocturnal values and are fairly evenly distributed within the valley as depicted in Fig. 11d. Since these PMCH tracer distributions were similar from one experiment to another it appears that the nocturnal flows near the bottom of this deep and narrow valley are generally well shielded from the external flows.

The behavior of the PDCH tracer, released at a height of 200 m above the valley floor, was similar to that of the PMCH tracer except for the elevated plume center and broader and more diffused distributions due to more extensive interactions with the ambient flows above the valley. The PMCP tracer released on the east ridgetop flowed directly into a small sidecanyon and subsequently into the Brush Creek Valley. The tracer remained primarily on the east side of the valley with the center of the plume situated about 200 m above the valley floor.

The ventilation rate of the tracers out of the valley during the morning transition period was evaluated by studying the rate of change of the surface tracer concentrations. After normalizing the concentrations for all tracer releases to a common release rate, one obtains the average rate of change of the concentrations shown by Curve A in Fig. 12. One may note that the concentrations are essentially constant prior to sunrise on the ridgetop. However, as the western sidewall is illuminated by the morning sun, the ventilation process is initiated within minutes as evidenced by the decrease in the tracer concentrations. This decrease is accelerated after the occurrence of sunrise on the valley floor due to the rapid venting of the tracers out of the valley. Approximately one to two hours after the ridgetop sunrise, the rate of ventilation of the valley atmosphere reached its maximum. At that time the tracer concentrations were reduced to about one-third of their levels prior to sunrise. The ventilation process continued as the east sidewall became exposed to the sun resulting in further decreases in the surface tracer concentrations. Note that the rate of decrease in the concentrations is independent of the time which the emissions ended. This suggests that the atmospheric dynamics that govern the rate of ventilation produces such strong mixing to completely override the effect of the continuing emissions. During the subsequent two hours, the concentrations continued to decrease to about 3% of their pre-sunrise levels due to further mixing of the valley atmosphere with the ambient flows.

Detailed analyses of the ventilation rates revealed some interesting fluctuations due to varying solar insolation, ambient meteorology, and the locations of the tracer plumes within the valley. By fractionating the data sets according to the meteorological conditions and plume exposure, curves B and C in Fig. 12 were derived. Curve B represents the average change in tracer concentrations during periods of strong solar insolation and high ambient flow conditions, while Curve C represents the periods with suppressed solar heating due to cloudy skies or tracer plumes situated within the eastern portion of the valley where they were shaded from the early sunshine. Even though the variations between the individual curves are not large, one may still note that for periods of strong solar heating and for tracer plumes situated closest to the western sidewall, the ventilation was initiated earliest after sunrise and progressed most rapidly. Likewise, periods characterized by strong ambient flows ventilated very rapidly. On the average Curve A in Fig. 12 shows that the ventilation process reduces the concentrations during the first hour after the ridgetop sunrise to 85% of their pre-sunrise levels and that in the subsequent three hours the concentrations drop to 36%, 10% and 3% of their respective nocturnal values.

## Suggested Methodology for Assessing Pollutant Dispersion in Valley Flows

On the basis of the experience gained from these studies, it is possible to provide guidance to an emergency response manager on a suggested approach that may be used to assess the potential impact of pollutants released from a facility situated within a valley environment. One may postulate that pollutant sources within a system of ridges and valleys may be located within three specific areas. These include the valley floor, the valley sidewalls and the ridgetops surrounding the valley. To assess the impact of pollutants released from a facility situated within one of these areas, one needs to evaluate the source emission characteristics, the ambient flows near the facility, and the general characteristics of the valley flow regimes througout the entire diurnal and seasonal cycles. With the nocturnal flows generally being associated with the most critical air quality scenario due to minimal pollutant mixing and trapping within valleys, the following measurements methodology may be suggested for defining the most significant features of the valley circulations from the standpoint of pollutant dispersion.

- An analysis of the topographic features with particular emphasis on topograpic constraints that may determine whether or not the valley is expected to drain or pool the nocturnal slope flows.

- Acquire vertical profiles of temperature and winds over the valley floor throughout the entire diurnal cycle to ascertain whether or not the valley drains or pools during the nighttime, the nature of the formation and break-up of the nocturnal inversion, and the growth of the daytime convective boundary layer.

- Acquire vertical profiles of temperature and winds on the valley sidewalls to evaluate the depth and strength of the slope flows relative to the expected emission height of pollutants released from slope situated facilities.

- Acquire climatological information on the wind and temperature structure over the valley floor, sidewalls, and the ambient flows over the valley to evaluate the frequency of occurrence of various valley circulations and their potential impact on atmospheric dispersion. This will include measurements of net radiation, soil moisture, temperature and cloud cover that will lead to estimation of the surface energy budget associated with various flow phenomena.

- Perform dispersion studies by releasing tracers from the facility site during the most critical valley circulation patterns from the standpoint of air quality impacts. This is particularly important for facilities situated on the ridgetop adjacent to a valley since it is difficult to predict under what conditions pollutants will be transported above the valley or be deflected into the valley.

This information in conjunction with air quality modeling will provide the emergency response manager with the predictive capability needed to estimate the impact of facility emissions on the valley environment.

## SUMMARY

This paper discusses the results acquired from several series of meteorological tracer experiments conducted by ASCOT scientists within the Anderson Creek Valley in The Geysers geothermal area in northern California and the Brush Creek Valley in western Colorado. These experiments were designed to evaluate the structure of the locally generated nocturnal slope and valley flows. The Anderson Creek Valley, which resembles a basin, exhibited shallow nocturnal slope flows on individual slopes near the ridges. These flows are characterized by a surface based inversion within the lowest 30 - 60 m of the atmosphere, and a downslope wind speed maximum at roughly half the depth of the inversion. These flows merge with those from other slopes, deepen upon descent into the valley, form a pool of cold air within the basin, and subsequently exits the valley through a terrain constricted opening. The depth of this pool generally varies between 100 and 300 m. This radiatively induced valley circulation may be strongly influenced by the ambient flows above the valley. Occasionally, westerly sea breezes or north-easterly flows over the ridges may intrude deeply into the valley to completely override the local circulations.

Measurements of the diurnal variation of net radiation at several sites within the Brush Creek Valley on clear days were strongly dependent on the slope and aspect angles of the sidewalls relative to the sun angle. The resulting daytime differential heating of opposing sidewalls produces a cross-valley flow that is especially important during the morning transition period. The nocturnal net radiative losses were typically 50 - 65 Wm-2 during clear nights. The valley sidewalls exhibited shallow nocturnal downslope flows with depths of typically less than 15 m. The nocturnal flows along the valley axis displayed a flow structure that may be characterized by a "Prandtl-parabolic wind field" description that includes a low-level jet along the valley center. Tracers released directly into the nocturnal downvalley flows revealed well-defined plume structures that were greatly influenced by differential solar heating of the valley surfaces during the morning transition period.

## Figure Captions

Fig. 1. Temperature distribution along a northwest-southeast cross-section of the Anderson Creek Valley.

Fig. 2. Flow lines of surface wind velocities within the Anderson Creek Valley during a period of strong nocturnal slope flows. The data were obtained for the period from 2300 - 2400 PST on September 19, 1980.

Fig. 4. Surface concentration pattern of PMCH perfluorocarbon tracer released directly into the nocturnal slope flows along the upper slopes of the Anderson Creek Valley. The one-hour release was initiated at 2300 PST on September 19, 1980. The concentrations are in units of ppt and are averaged over the first two-hour period after the initiation of the release. The release rate was 0.12 g/s.

Fig. 3. A northeast-southwest cross-section of the Anderson Creek Valley showing gradual incursion of northeast winds into the valley on September 22, 1980. The contours indicate the position of the bottom of the transition layer across the valley at the indicated times (PST).

Fig. 5. Net all-wave radiation flux ($Q^*$), soil heat flux ($Q_G$), latent heat flux ($Q_E$) and sensible heat flux ($Q_H$) for five sites within the Brush Creek Valley, September 25, 1984.

Fig. 6. Vertical profiles of winds above the northeast sidewall of the Brush Creek Valley during the nocturnal, morning transition and daytime periods on September 30, 1984.

Fig. 7. Cross-valley views of the flows observed on September 30, 1984 within the Brush Creek Valley. The data were obtained during (a) the nocturnal, (b) the morning transition, and (c) the daytime periods. Positive values denote the downvalley flows while negative values indicate upvalley flows in units of m/s.

Fig. 8. The median of the hourly-averaged sigma theta values (top) and wind speeds (bottom) acquired from measurement sites within the Brush, Anderson, and Big Sulphur Creek Valleys.

Fig. 9. Nocturnal average (2300 - 0600 MST) downvalley flow depth within the Brush Creek Valley as a function of the averaged Angstrom ratio.

Fig. 10. A plot of the height of the bottom of the transition layer as a function of total wind speed at ridge height. The data were obtained at several locations within the Brush Creek Valley at various times. The wind directions at the ridgetop are

denoted by arrows in the direction of the wind.

Fig. 11. Distributions of the PMCH tracer measured within the Brush Creek Valley on September 30, 1984. Figures (a), (c), and (d) provide representative vertical cross-sections of the tracer concentrations near the mouth of the valley during the nocturnal, morning transition, and daytime periods, respectively. The west side of the valley is on the left. Figure (b) provides an along valley axis cross-section of the nocturnal concentration distribution. The concentration units are in ppt. The data were obtained between 0200 -0300 MST (nocturnal), 0700-0800 MST (morning transition), and 1000-1100 MST (daytime) periods.

Fig. 12. Tracer concentrations within the Brush Creek Valley during the morning transition period.

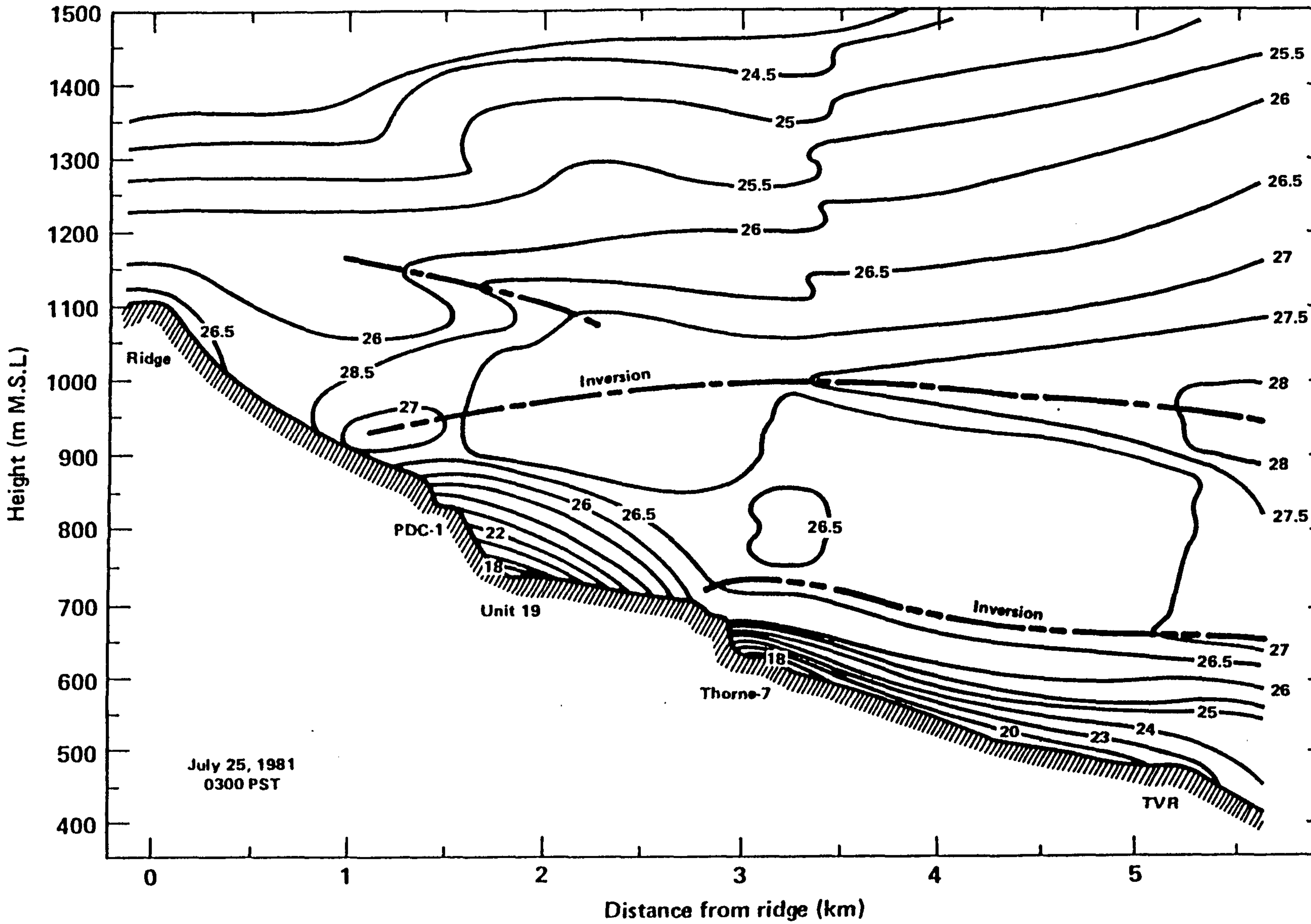
1500
1400
1300
1200
1100
1000
900
800
700
600
500
400
Height (m M.S.L)
0
1
2
3
4
5
6
Distance from ridge (km)
24.5
25
25.5
26
26.5
27
27.5
28
28.5
22
18
20
23
24
Inversion
Ridge
PDC-1
Unit 19
Thorne-7
TVR
July 25, 1981
0300 PST

Fig. 2

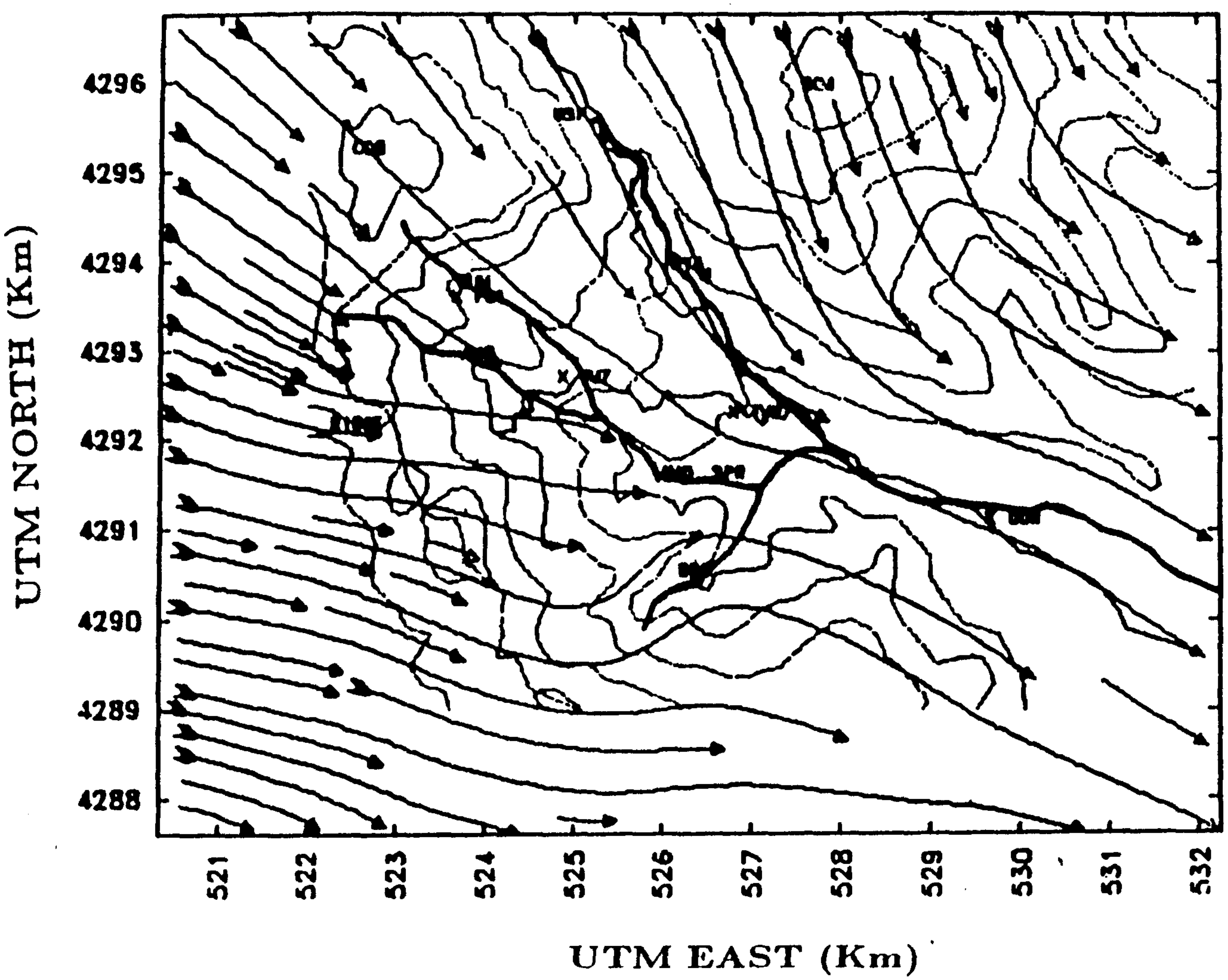

4296
4295
4294
4293
4292
4291
4290
4289
4288
521
522
523
524
525
526
527
528
529
530
531
532
UTM NORTH (Km)
UTM EAST (Km)


Fig. 2

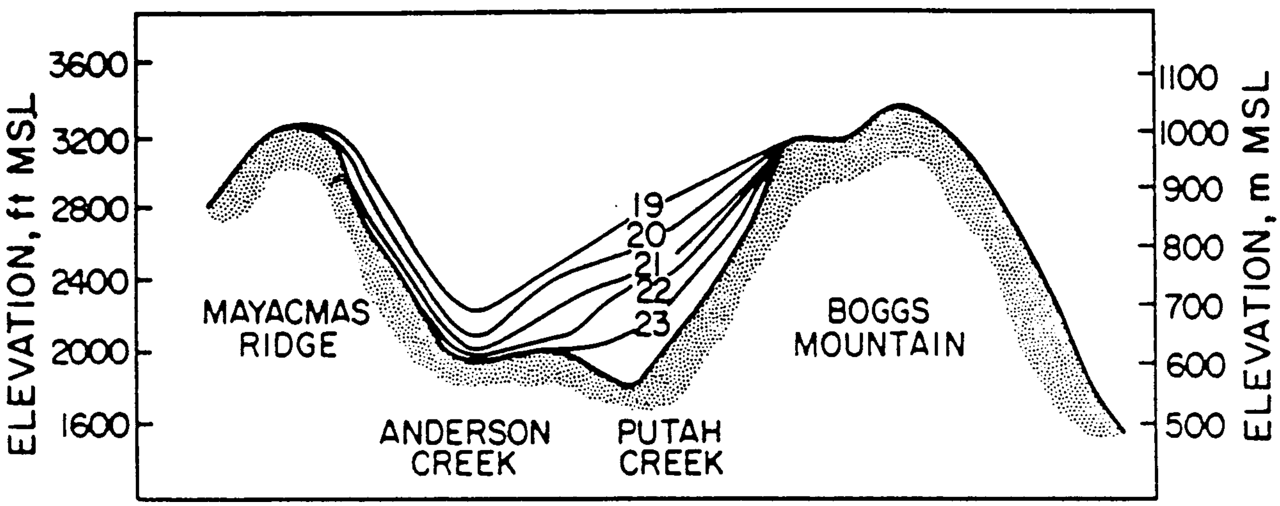


Cross section parallel to external wind direction showing gradual incursion of NE winds into the valley (September 22, 1980).

Fig. 3

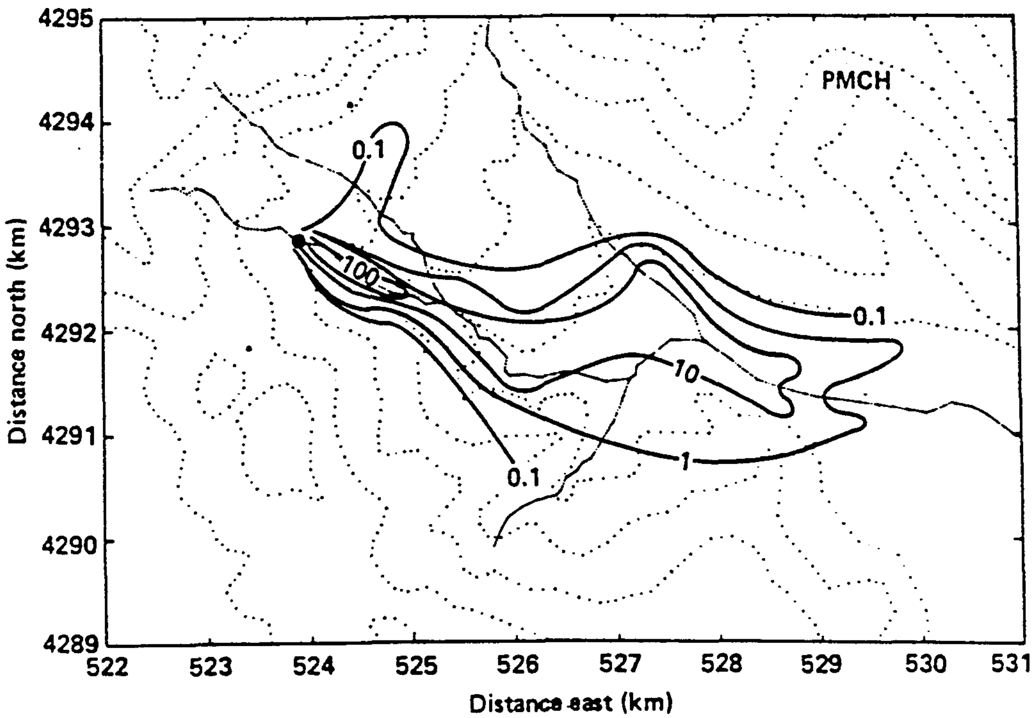

PMCH
0.1
100
10
1
0.1
0.1
4295
4294
4293
4292
4291
4290
4289
Distance north (km)
522
523
524
525
526
527
528
529
530
531
Distance east (km)


Fig. 4.

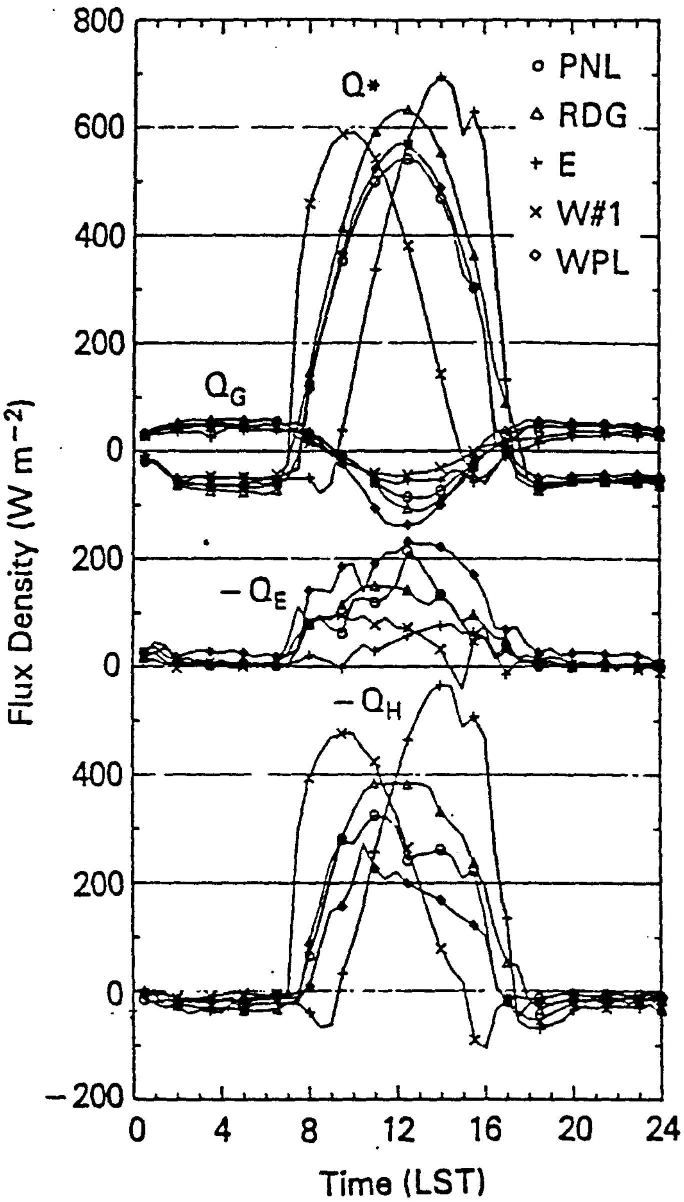

800
600
400
200
0
200
0
400
200
0
−200
Q*
○ PNL
△ RDG
+ E
× W#1
◇ WPL
$Q_G$
$-Q_E$
$-Q_H$
Flux Density (W m$^{-2}$)
0
4
8
12
16
20
24
Time (LST)


Fig. 5.

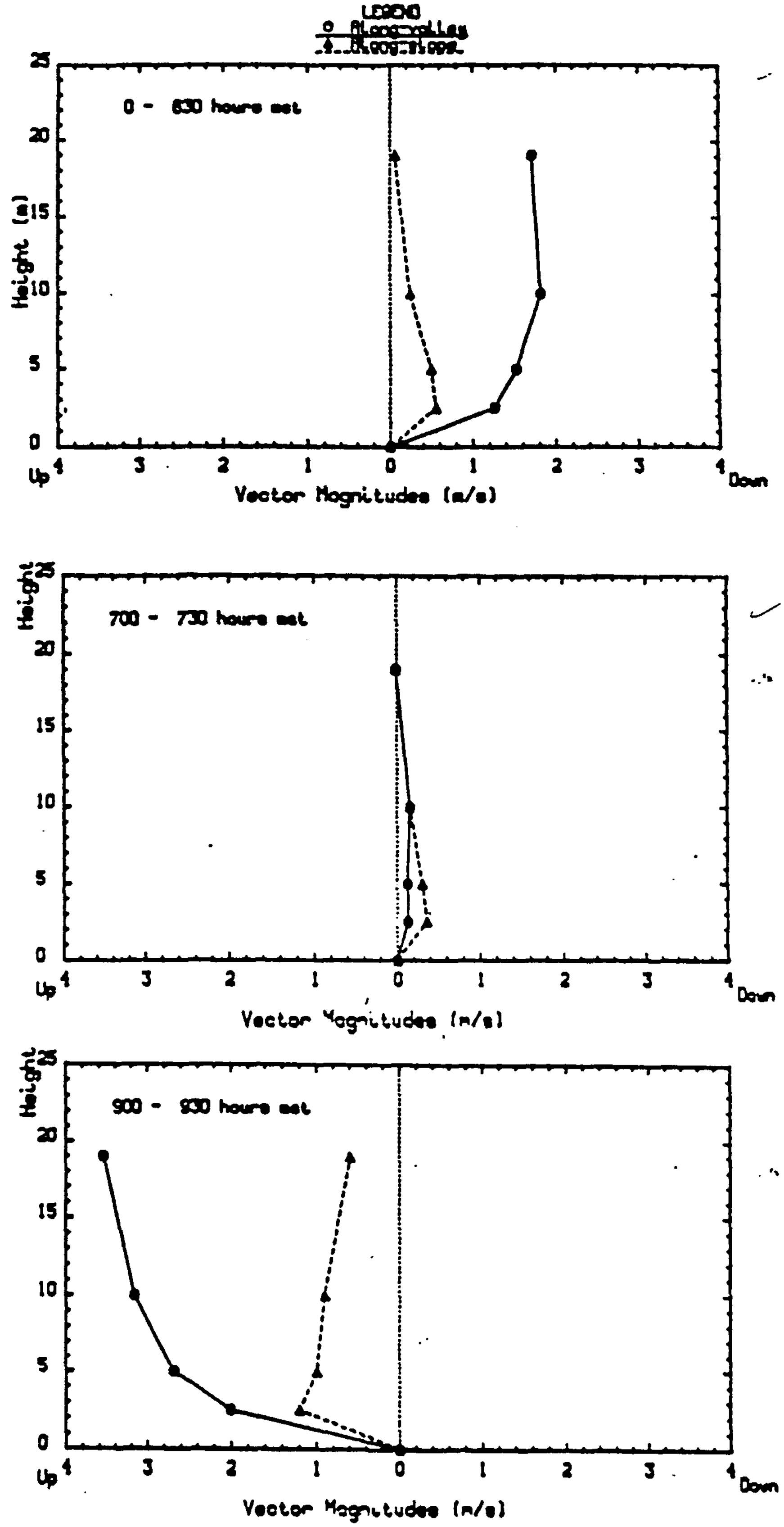
LEGEND
Height (m)
Vector Magnitudes (m/s)
Up
Down
700 - 730 hours mst
Height
Vector Magnitudes (m/s)
900 - 930 hours mst
Height
Vector Magnitudes (m/s)

Fig. 6

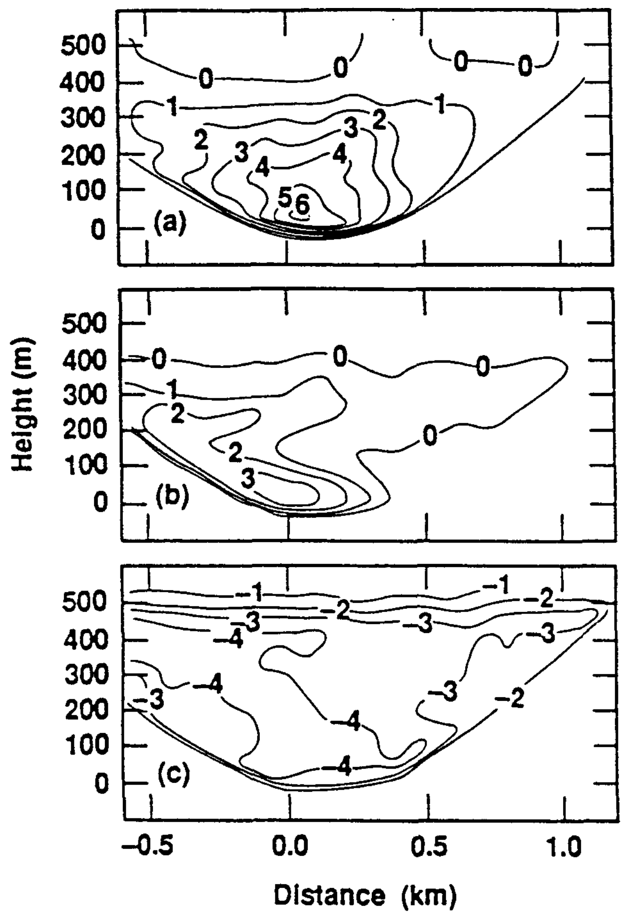


Fig. 7

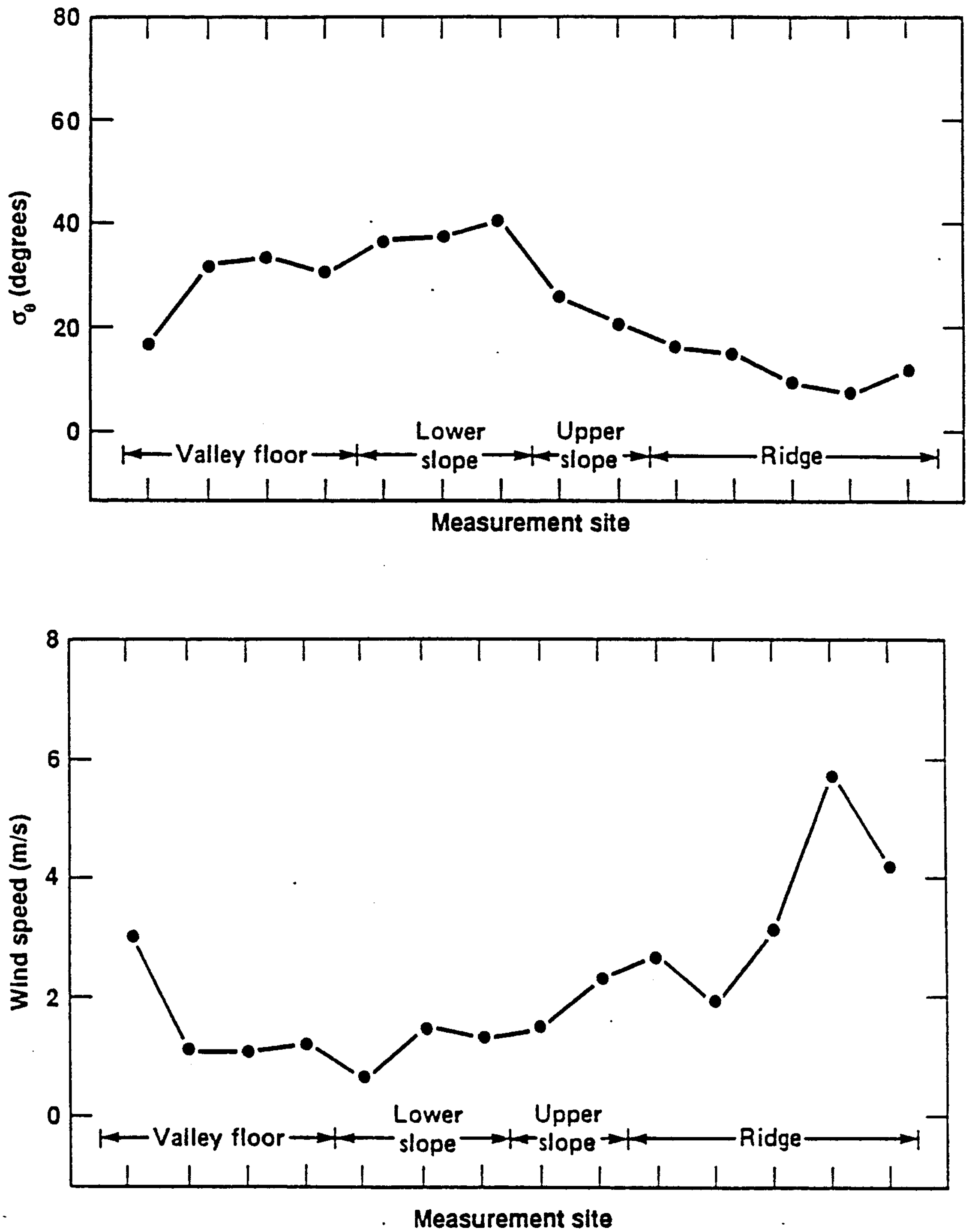
80
60
40
20
0
σθ (degrees)
Valley floor
Lower slope
Upper slope
Ridge
Measurement site
8
6
4
2
0
Wind speed (m/s)
Valley floor
Lower slope
Upper slope
Ridge
Measurement site

Fig. 8

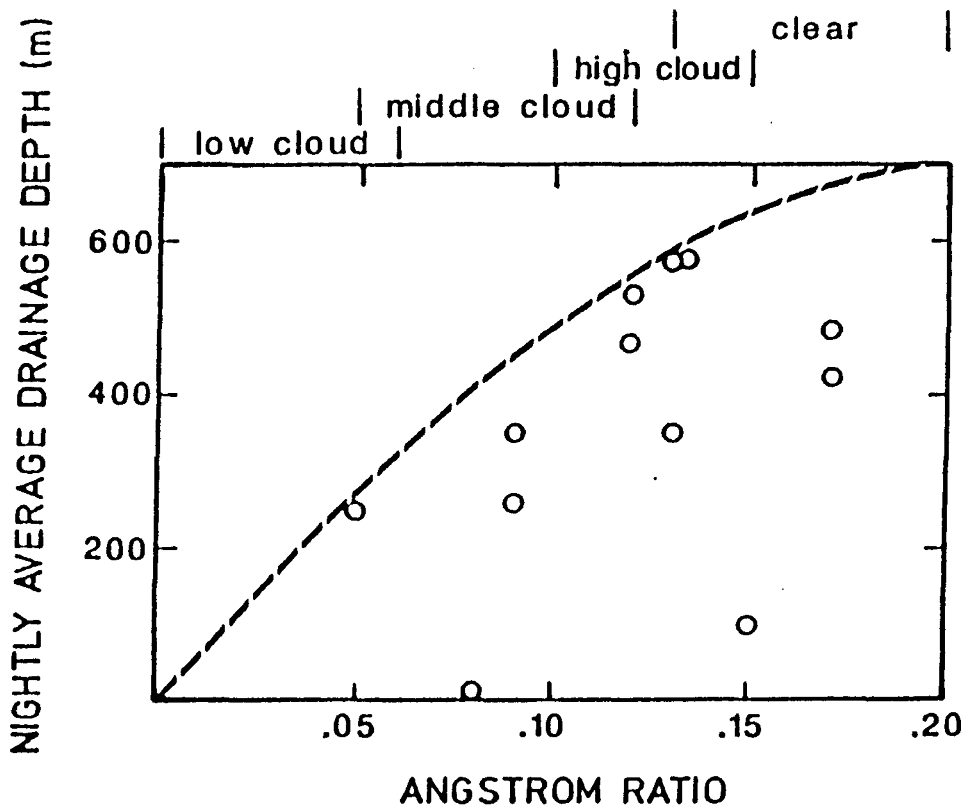

low cloud
middle cloud
high cloud
clear
NIGHTLY AVERAGE DRAINAGE DEPTH (m)
600
400
200
.05
.10
.15
.20
ANGSTROM RATIO


Fig. 9

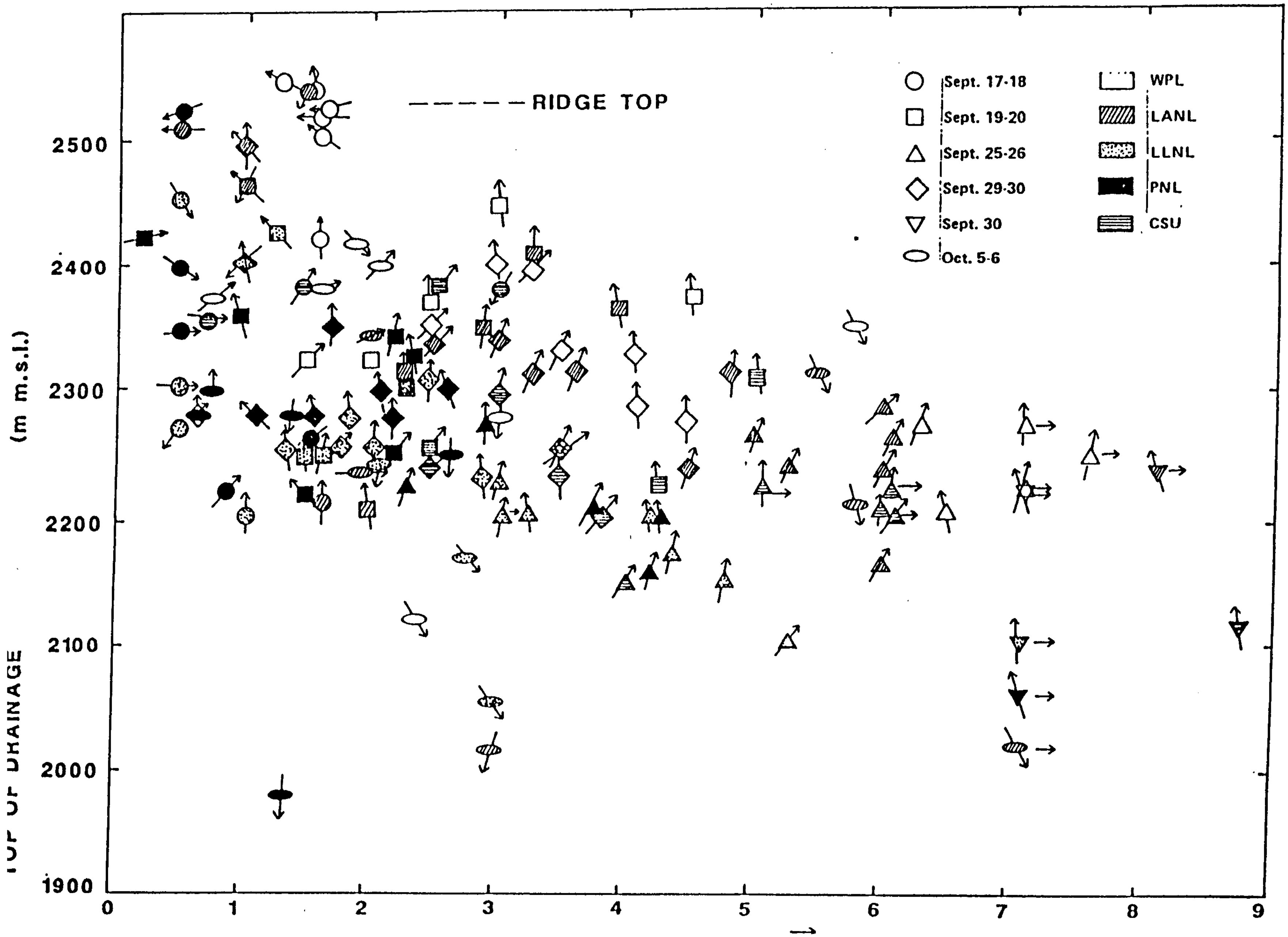
RIDGE TOP
Sept. 17-18
Sept. 19-20
Sept. 25-26
Sept. 29-30
Sept. 30
Oct. 5-6
WPL
LANL
LLNL
PNL
CSU
2500
2400
2300
2200
2100
2000
1900
0
1
2
3
4
5
6
7
8
9
(m m.s.l.)

Fig. 10

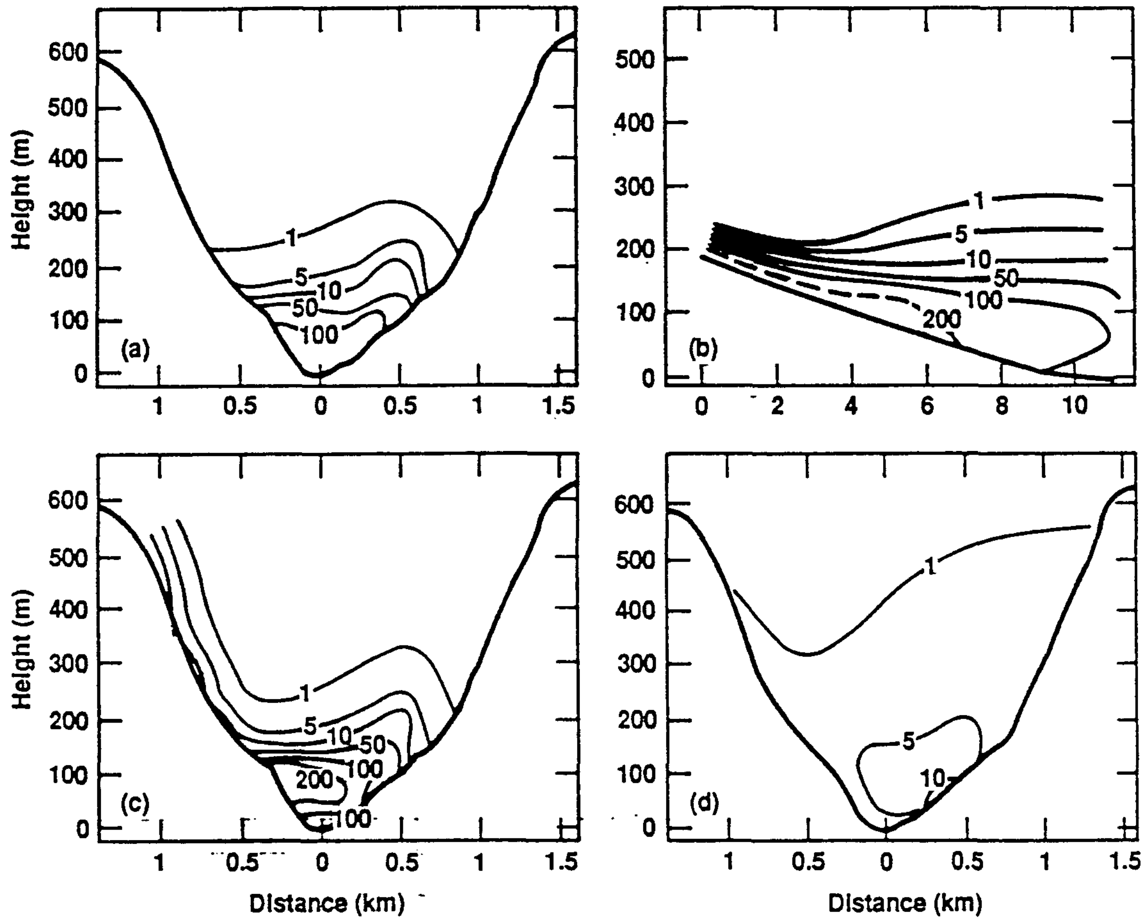

Height (m)
600
500
400
300
200
100
0
(a)
1
5
10
50
100
1
0.5
0
0.5
1
1.5
500
400
300
200
100
0
(b)
1
5
10
50
100
200
0
2
4
6
8
10
(c)
200
100
Distance (km)
(d)
Distance (km)


Fig. 11.

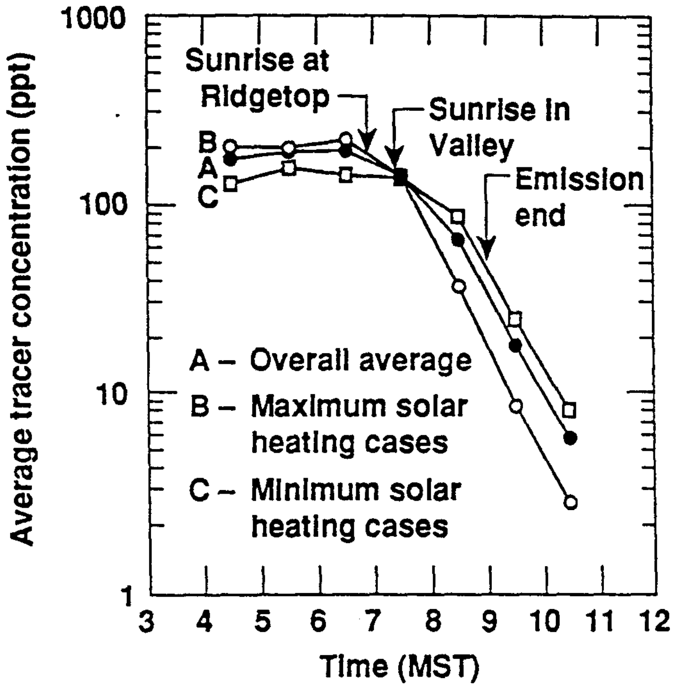
1000
100
10
1
Average tracer concentration (ppt)
Sunrise at Ridgetop
Sunrise in Valley
Emission end
B
A
C
A – Overall average
B – Maximum solar heating cases
C – Minimum solar heating cases
3 4 5 6 7 8 9 10 11 12
Time (MST)

Fig. 12